Electronic Supplementary Material (ESI) for Journal of Materials Chemistry A.

Supporting Information

Removing the Barrier to Water Dissociation on Single-Atom Pt Sites Decorated with a CoP Mesoporous Nanosheet Array to Achieve Improved Hydrogen Evolution

Shenghua Ye, Wei Xiong, Peng Liao, Lirong Zheng, Xiangzhong Ren, Chuanxin He, Qianling Zhang and Jianhong Liu

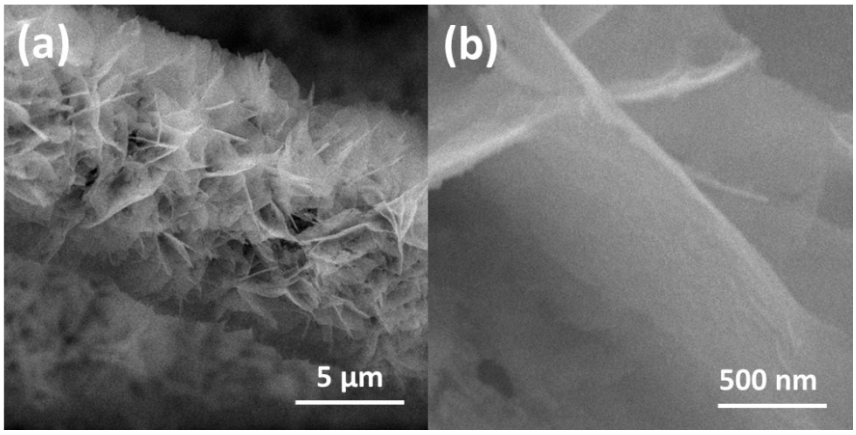

Figure S1. SEM images of $Co(OH)_2$ NSs/CFC.

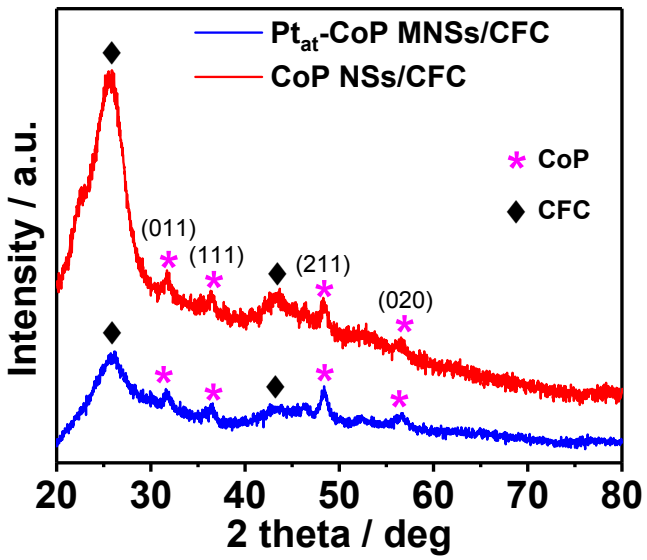

Figure S2. XRD patterns of Pt_{at}-CoP MNSs/CFC and CoP NSs/CFC (PDF #29-0497).

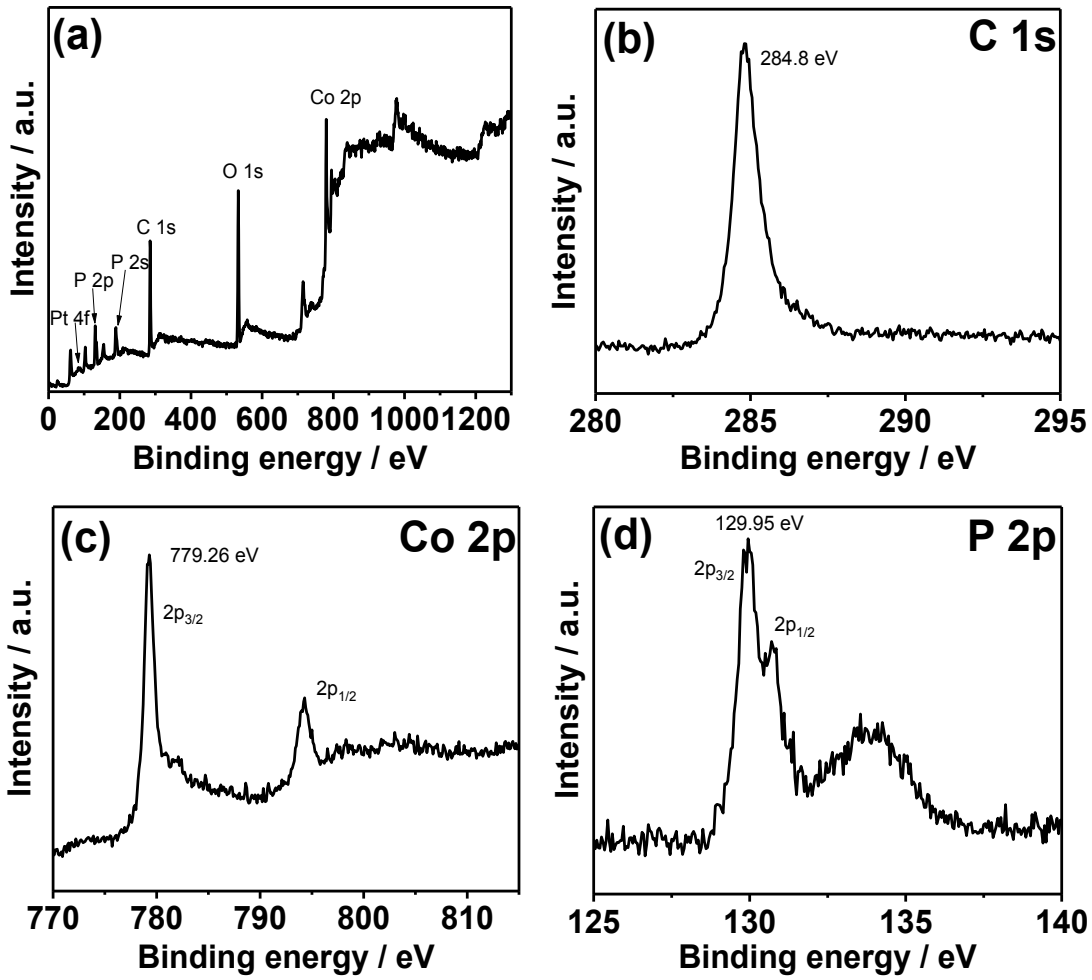

Figure S3 XPS: (a) survey, (b) C 1s, (c) Co 2p, and (d) P 2p of Pt_{at}-CoP MNSs/CFC.

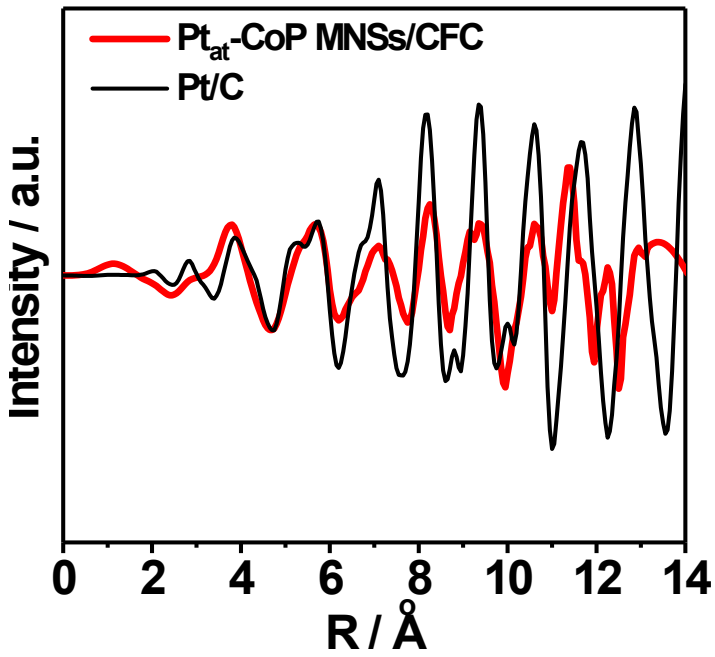

Figure S4. Pt L_3-edge EXAFS oscillation of Pt-CoP MNSs/CFC and Pt/C.

Table S1 EXAFS fitting parameters at the Pt L_3-edge for various samples.

Sample	Shell	CN[a]	R (Å)[b]	σ^2 (Å^2·10^3)[c]	ΔE_0 (eV)[d]	R factor (%)
Pt$_{at}$-CoP MNSs/CFC	Pt-P	6.0	2.26	14.0	-1.0	0.4
Pt/C	Pt-Pt	12.0	2.76	5.0	8.5	2.4

[a]CN: coordination numbers; [b]R: bond distance; [c]σ^2: Debye–Waller factors; [d]ΔE_0: inner potential correction; R factor: goodness of fit.

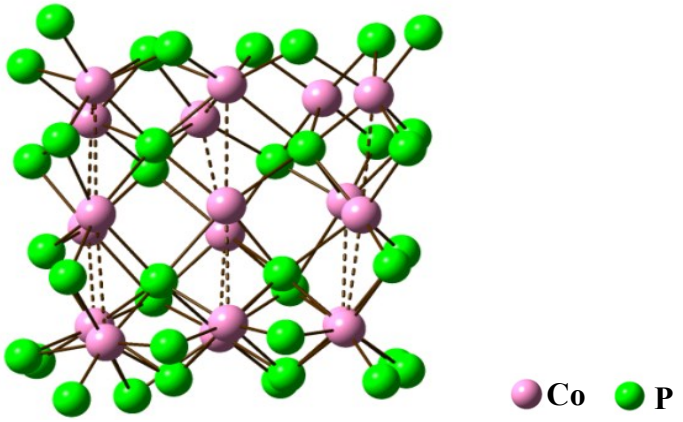

Figure S5. CoP crystal structure viewed down the b axis (The pink spheres are Co atoms and the green spheres are P atoms. The dashed lines indicate the metal–metal bonding network).

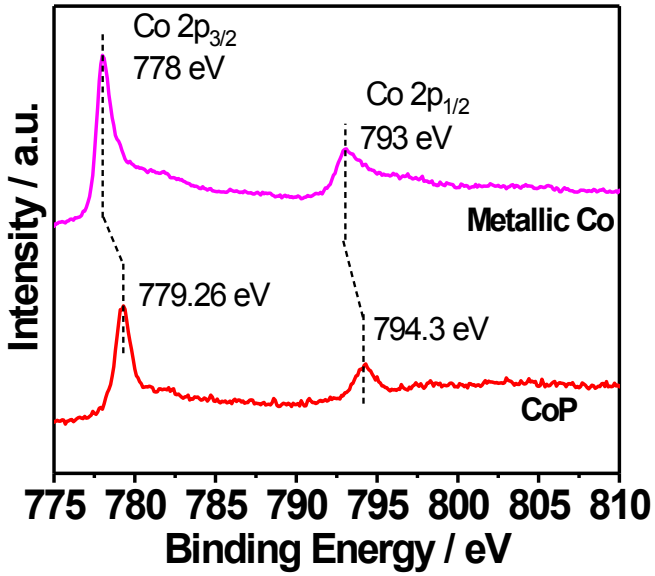

Figure S6. XPS spectra of Co 2p in CoP nanosheets and metallic Co.

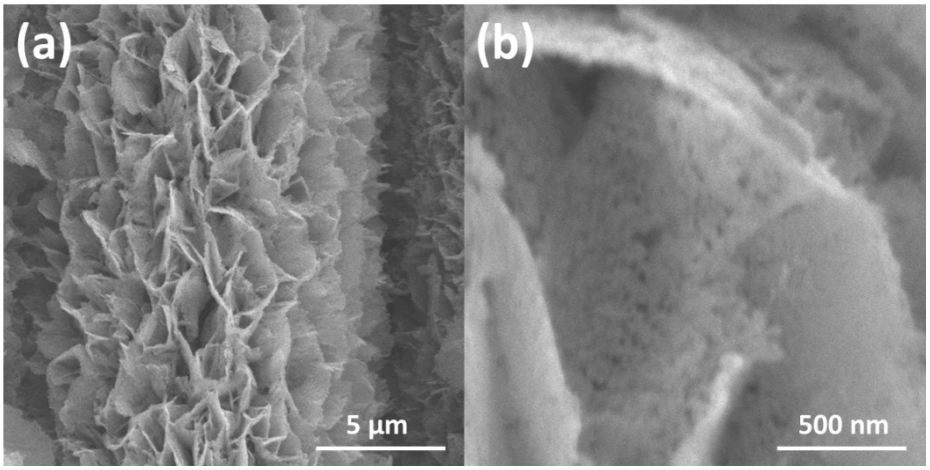

Figure S7. SEM image of CoP NSs after immersion in a 12 mM HCl solution.

Table S2. HER performances of Pt_{at}-CoP MNSs/CFC and other reported single-atom catalysts in alkaline media.

Catalyst	Loading of metal / wt%	Onset potential /mV	overpotential at 10 mA cm^{-1} / mV after iR correction	Tafel slope / mV deg^{-1}	Ref.
Pt_{at}–CoP MNSs/CFC	**0.7**	**~0**	**13**	**30.28**	**This work**
Pt/np-$Co_{0.85}Se$	1.03	~0	20	-	*Nat. Commun.* **2019**, *10*, 1743
Ru_{SA}-N-S-$Ti_3C_2T_x$	1.2	~0	76	90	*Adv. Mater.* **2019**, *1903841*
Ru-NC-700	4	~0	12	-	*Nat. Commun.* **2019**, *10*, 631.
RuAu-0.2	15.35	-	24	37	*Adv. Energy Mater.* **2019**, *1803913*
SA-Ru-MoS_2	5	~0	76	21	*Small Methods* **2019**, 1900653
SANi-I	1.2	-	-	34.6	*Angew. Chem. Int. Ed.* **2019**, *58*, 12252
Pt@PCM	0.53	~0	139	73.6	*Sci. Adv.* **2018**. *4*, eaao6657
W-SAC	1.21	-	85	53	*Adv. Mater.* **2018**, *1800396*
$Mo_1N_1C_2$	1.32	13	132	90	*Angew. Chem. Int. Ed.* **2017**, *56*, 16086
PtSA-NT-NF	1.76	~0	~70	-	*Angew. Chem. Int. Ed.* **2017**, *56*, 13694.
Co-G	-	~200	~280	-	*Nat. Commun.* **2015**, *6*, 8668.
Ni-C-N	-	~40	30.8	40	*J. Am. Chem. Soc*. **2016**, *138*, 14546
np-$Cu_{53}Ru_{47}$	-	~0	15	30	*ACS Energy Lett.* **2020**, *5*, 192
Ru@MWCNT	12.8	~0	17	27	*Nat. Commun.* **2020**, *11*, 1278
Co-substituted Ru	-	~0	13	29	*Nat. Commun.* **2018**, *9*, 4958
NiO-1TMoS_2/CFP	-	-	46	52	*Nat. Commun.* **2019**, *10*, 982
Pt_1/N-C	2.5	~0	46	36.8	*Nat. Commun.* **2020**, *11*, 1029
Ni_5P_4 - Ru	3.83	17	54	52.0	*Adv. Mater.* **2020**, *32*, 1906972
PtSA@BP	2.5	~0	26	37	*J. Mater. Chem. A* **2020**, *8*, 5255
PtRh DNAs	-	~0	28	47	*Int. J. Hydrogen. Energy* **2020**, *45*, 6110
NRAS	2	-	72	193	*ACS Appl. Mater. Interfaces*, **2020**, *12*, 7057
Co_1/PCN	0.3	36	138	52	*Nat. Catal.* **2019**, *2*, 134

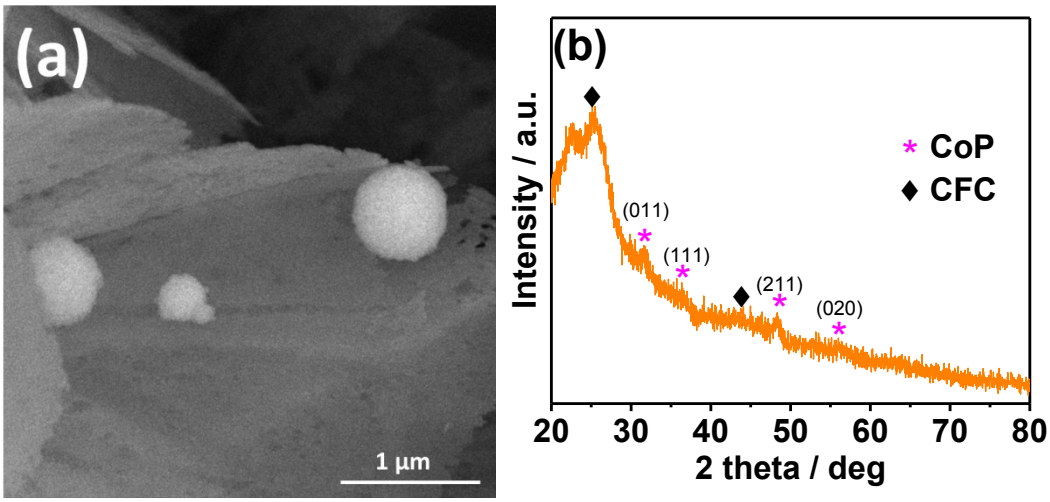

Figure S8. (a) SEM image and (b) XRD pattern of Pt@CoP NSs/CFC.

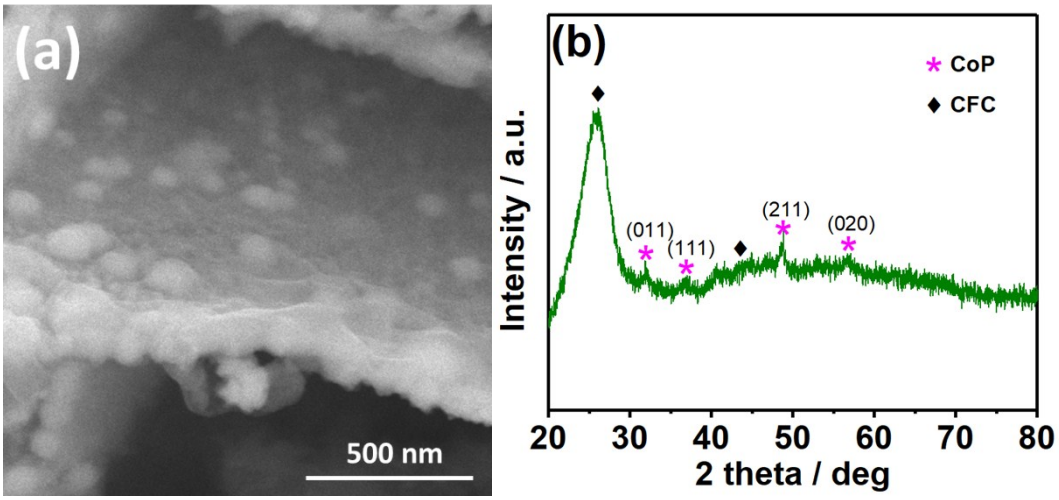

Figure S9. (a) SEM image and (b) XRD pattern of Pd@CoP NSs/CFC.

Pt@CoP NSs/CFC and Pd@CoP NSs/CFC are synthesized by eletrodepositing Pt and Pd on CoP NSs/CFC in the bath of H_2PtCl_6 and K_2PdCl_4 solution for 30min. Particularly, large amounts of Pt leached off from the electrode during the electrodeposition, the content of Pt is as low as 2.36 wt% measured by ICP-AES, large and sparse Pt nanoparticles anchored on the CoP NSs could be observed as shown in Figure S8a, this phenomenon may be attributed to weak adhesive force between Pt and CoP. There isn't any diffraction peak assigned to metallic Pt found in the XRD pattern as shown in Figure S8b, it means that the Pt nanoparticles anchored on CoP NSs are amorphous. On the contrary, the small and dense Pd nanoparticles could be identified on the CoP NSs (Figure S9a), and the content of Pd is 13.82wt% measured by ICP-AES, suggesting the stronger adhesive force between Pd and CoP. There isn't any diffraction peak assigned to metallic Pd found

in the XRD pattern shown in Figure S9b, indicating that the Pd nanoparticles anchored on CoP NSs are amorphous, which is in accordance with the previous literarure.[1]

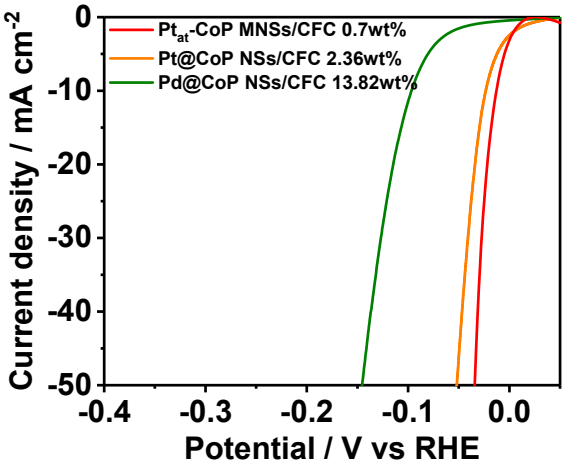

Figure S10 LSV curves of Pt$_{at}$–CoP MNSs/CFC, Pt@CoP NSs/CFC, and Pd@CoP NSs/CFC in 1 M KOH solution at 2mV/s after iR correction.

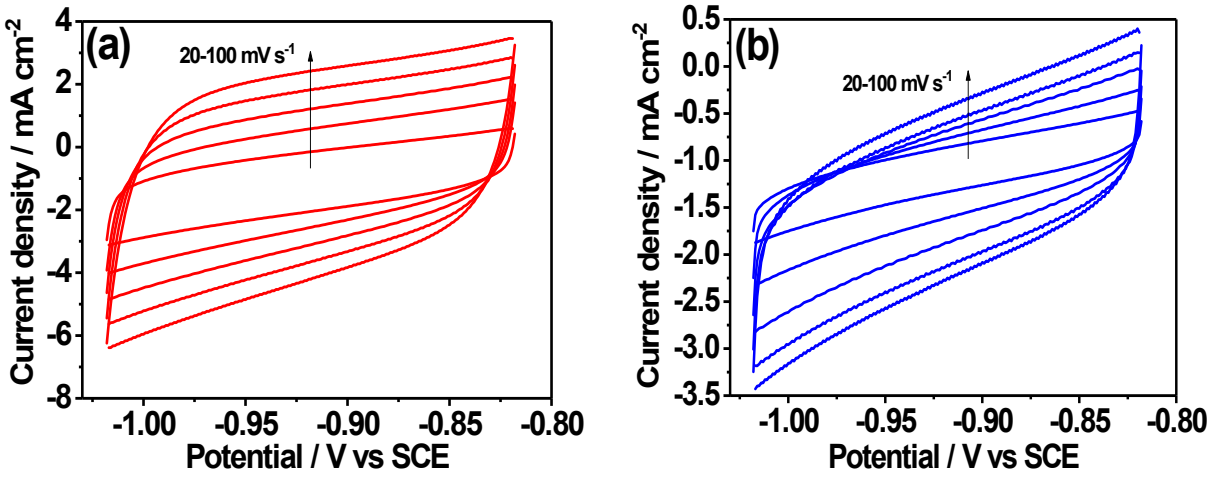

Figure S11. CVs of (a) Pt$_{at}$–CoP MNSs/CFC and (b) CoP NSs/CFC in a 1.0M KOH solution at scan rates of 20, 40, 60, 80, and 100mV/s.

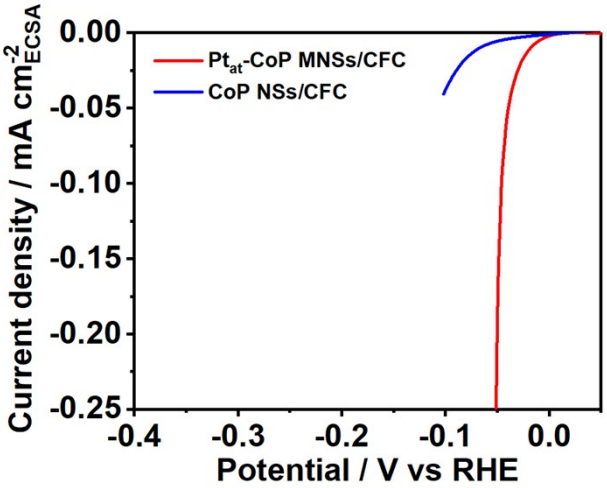

Figure S12 LSV curves of Pt_{at}–CoP MNSs/CFC and CoP NSs/CFC in a 1.0 M KOH solution with current density normalized to the ECSA determined by the C_{DL}.

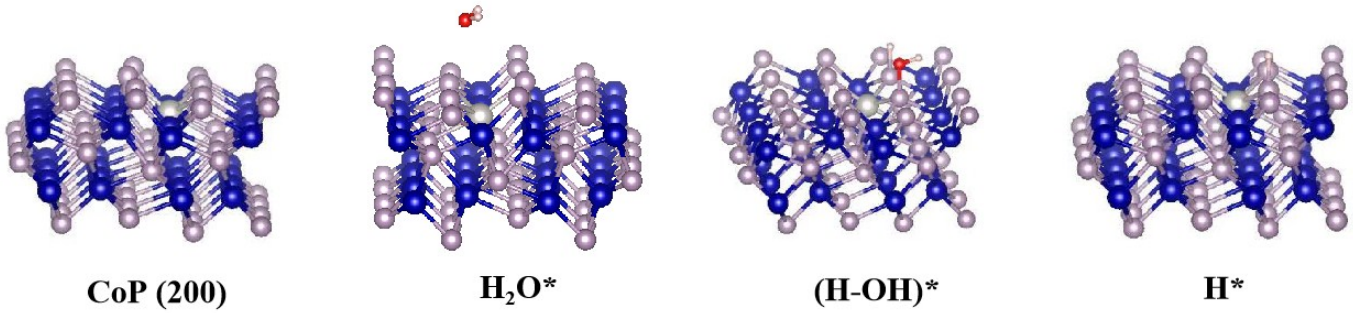

Figure S13 Calculation models of the CoP (200) facet and the intermediates H_2O*, (H-OH)*, and H* adsorbed on the Co sites.

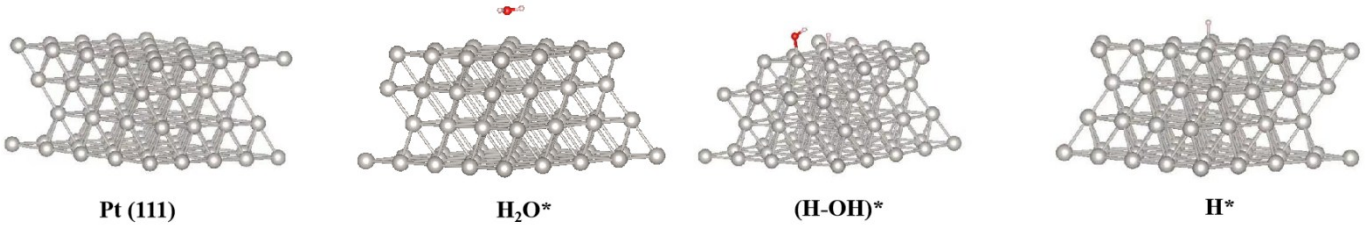

Figure S14 Calculation models of the Pt (111) facet and the intermediates H_2O*, (H-OH)*, and H* adsorbed on the Pt sites.

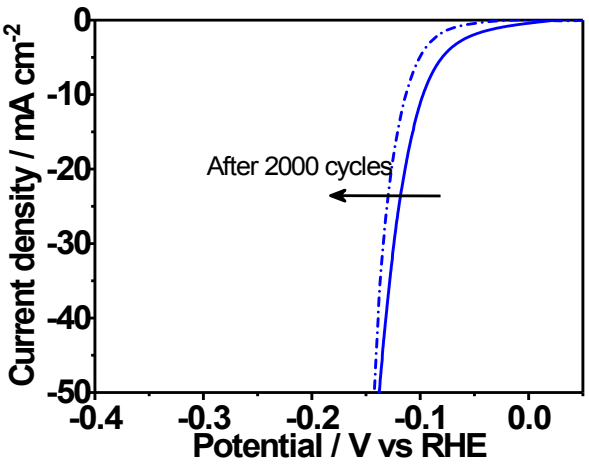

Figure S15. LSVs of CoP NSs/CFC in 1.0M KOH before and after 2000 cycles.

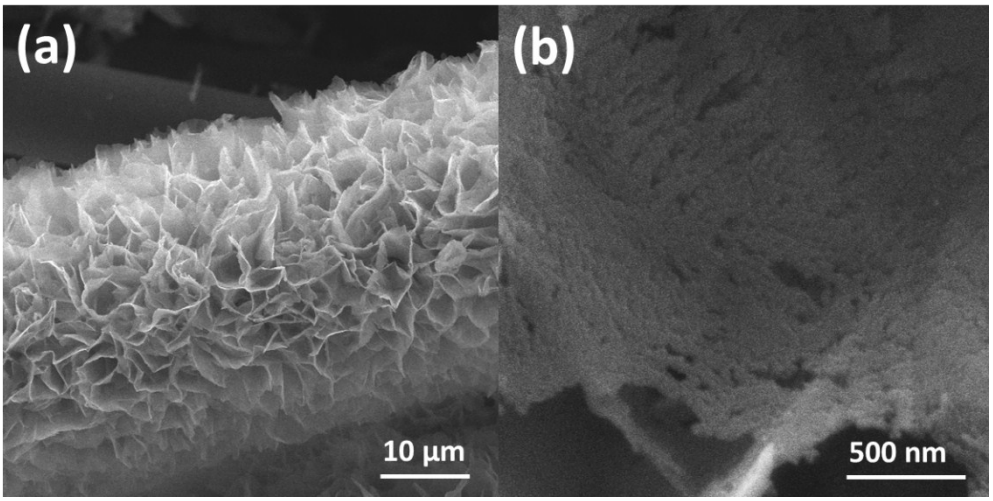

Figure S16. SEM image of Pt_{at}-CoP MNSs/CFC after the durability test.

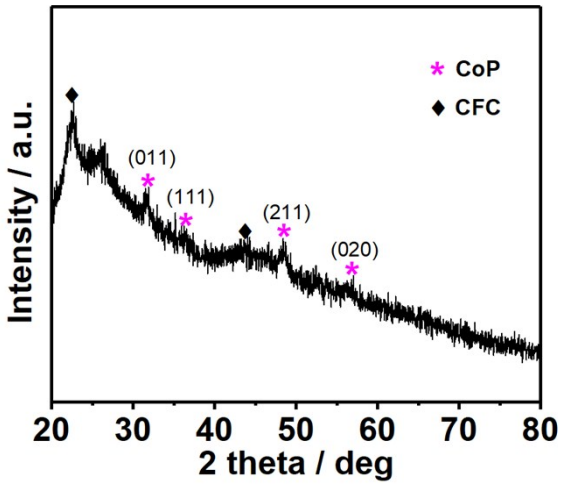

Figure S17 XRD pattern of Pt_{at}-CoP MNSs/CFC after the durability test.

Reference

[1] S. H. Ye, J. X. Feng, G. R. Li. *ACS Catal.* 2016, **6**, 7962-7969.